An Aeroacoustic Model for High-Speed, Unsteady Blade-Vortex Interaction

Rudolph Martinez* and Sheila E. Widnall†
Massachusetts Institute of Technology, Cambridge, Massachusetts

A three-dimensional aeroacoustic model is developed to predict the sound pulse radiated by the passage of a helicopter blade over a potential vortex. The linearized analysis assumes that either the blade-vortex separation is small or that the blade-tip Mach number is close to 1, or both, so that an acoustically noncompact situation exists. The three-dimensional blade loading due to blade-vortex interaction is constructed through a spanwise superposition of two-dimensional solutions with strength linearly increasing from hub to tip. Such a loading overestimates somewhat the strength of tip region dipoles in the acoustic calculation that follows. The final expression for the predicted far-field signature is obtained in closed form, and thus permits a relatively inexpensive calculation of the directivity of peak acoustic pressures in three dimensions.

Nomenclature

a = $\sqrt{-\mu^2}$ for $\mu^2<0$
arg = argument, or phase, of a complex number
b = blade semichord, reference length
c_0 = dimensional sound speed
C = complex constant, Eqs. (28) and (29)
h = nondimensional vertical blade-vortex separation
Im = imaginary part of a complex number
K = $k_x M/(1-M^2)$
k_x = reduced frequency or nondimensional chordwise wave number
k_y = $k_x \tan\Lambda$, the spanwise wave number
L = nondimensional blade length
M = freestream Mach number and blade-tip Mach number in three-dimensional theory
M_{eff} = effective Mach number, $M/\sin\Lambda$
P,P_* = perturbation pressures, Eqs. (6) and (15), respectively
$\bar{P}$ = Fourier transform of P_*, Eq. (19b)
p = predicted pulse
r = nondimensional distance to observer
$\bar{r}$ = nondimensional vector position of observer
Re = real part of a complex number
t = dimensional time
U = dimensional freestream velocity, or blade-tip velocity
W = Fourier transform of vortex-induced upwash
w_0 = $W/\cos\Lambda$
w = dimensional vortex upwash
x,y,z = chordwise, spanwise, and normal to blade nondimensional spatial coordinates
Y,Z = $\sqrt{1-M^2}y$, $\sqrt{1-M^2}z$
Λ = blade-vortex interaction angle
μ = frequency parameter, Eq. (8)
ξ = $x_a\cos\Lambda + y\sin\Lambda$
ρ_0 = freestream density
ω = acoustic frequency
Ω = rotor angular velocity
ϕ,γ = angles in spherical coordinate system fixed in the still fluid, Fig. 3
Γ = dimensional vortex strength
θ = $\tan^{-1} Z/x$
τ = $t - br_a/c_0$, retarded time

Subscripts

a = acoustic reference frame
2-D = two-dimensional solution
3-D = three-dimensional solution

Superscripts

$(\ )^*$ = complex conjugate

Introduction

THE accurate prediction of aerodynamically generated noise from rotating blades continues to be a goal for designers of gas turbines and helicopter rotors. The present paper reports on a new model developed to predict the acoustic pulse radiated as a result of blade-vortex interaction for a helicopter rotor with high subsonic tip Mach number.

Aeroacoustic noncompactness in blade-vortex interaction occurs whenever either of the following two conditions is present, or when they are both present simultaneously: 1) the vertical blade-vortex separation hb is small in comparison to the semichord b; and 2) the blade-tip Mach number M has a high subsonic value. For acoustic purposes, the surface of the blade may be thought of as a flat continuous sheet of dormant acoustic dipoles that are suddenly stimulated by local interaction with the passing vortex. Each point on the surface then emits an elementary acoustic pulse that, by Fourier's theorem, may be broken down into a spectrum of tones. In a chordwise noncompact situation, two tones of identical frequency ω, fired at different retarded times $(t-br/c_0)_1$ and $(t-br/c_0)_2$ by two distinct dipoles located at the same spanwise station, may arrive at the far-field observer point br simultaneously at time t. The condition $\Delta(t-br/c_0) \ll 2\pi/\omega$, the criterion for acoustic compactness, is not met; $2\pi/\omega$ denotes the tones' period of oscillation. A high-aspect-ratio planform that is chordwise noncompact is also automatically spanwise noncompact, whereas the converse is not true.

Widnall[1] has developed a model to predict noise due to blade-vortex interaction for a loading that is chordwise compact, but not necessarily spanwise compact. Filotas' aerodynamic theory[2] was used to predict the lift harmonics needed for the acoustic calculation. In the same work, she discussed in detail the important role played by the interaction angle Λ in the model for the acoustic field: for $\sin\Lambda < M$ strong radiation from the whole blade surface is present, whereas for $\sin\Lambda > M$ only a relatively weak field due to finite-span effects is given off. Physically, for $\sin\Lambda < M$ unsteady load fronts due to blade-vortex interaction travel supersonically through the still fluid; for $\sin\Lambda > M$ they have a subsonic trace speed.

Received Feb. 23, 1982; revision received Oct. 1, 1982.

*Post-Doctoral Research Associate, Department of Aeronautics and Astronautics; currently with Cambridge Acoustical Associates, Inc., Cambridge, Mass. Member AIAA.

†Professor, Department of Aeronautics and Astronautics. Associate Fellow AIAA.

At high speeds, and/or for small vertical blade-vortex separation, use of Filotas' incompressible flow model to determine unsteady loadings is not valid. For this operating regime the proper aeroacoustic theory must include the effects of compressibility and high frequency normally neglected at low speeds. Therefore, the theory developed here does not replace or generalize any of the previously cited compact models; rather, it attempts to complement them by investigating a flight regime for which they do not hold.

Mathematically, noncompactness results in the blade surface pressure distribution becoming inextricably coupled to its acoustic field. For this reason, the authors in Ref. 3 developed a unified aerodynamic-acoustic two-dimensional theory for a flat-plate airfoil passing through a gust; the gust represented a wave number component of the nonuniform upwash induced on the airfoil surface by a vortex. A result of that work was an expression for the pressure at a general field point (x,z) that checked, for $z=0$, with airfoil loadings previously predicted by Adamczyk[4] and Amiet.[5]

Reference 3 discussed in detail how and why Landahl's[6] concept of separating the effects of the leading and the trailing edges is useful in the calculation of a noncompact loading on an infinite-span airfoil. Briefly, his technique takes advantage of the rapid $1/\sqrt{k_x x/(1-M^2)}$ decay of the loading computed by neglecting the trailing edge in the problem; such a solution violates the Kutta condition and $\Delta p=0$ across the wake by only a small amount. Since the correct loading over most of the airfoil should then not be very different from that given by the leading-edge solution, satisfying the Kutta condition introduces a small correction that is important, for $k_x/(1-M^2)\gg 1$, only near the trailing edge. Therefore, the edges behave physically as independent sources of sound and unsteady loading.

The analysis presented here essentially starts with the leading-edge contribution to the pressure field derived in Ref. 3 for a two-dimensional (infinite-span) flat-plate airfoil passing through an oblique gust. This leading-edge solution is given initially in terms of a complex-contour integral that, as shown, can be evaluated to give a simple expression for the pressure field everywhere. The result agrees with that obtained by approximating the integral in the far field (the tone radiation in two dimensions), say by the method of steepest descents; yet, it holds not just for $\sqrt{x^2+Z^2}\to\infty$, but at all spatial positions. In fact, the loading on the airfoil surface due to the passage through the gust may be found by letting $\theta=0$ in that expression. We find the two-dimensional aerodynamic problem of a leading edge passing subsonically through a gust reminiscent of the classical Sommerfeld diffraction problem of a wave incident on a semi-infinite flat plate; the latter also has a relatively simple closed-form solution everywhere.

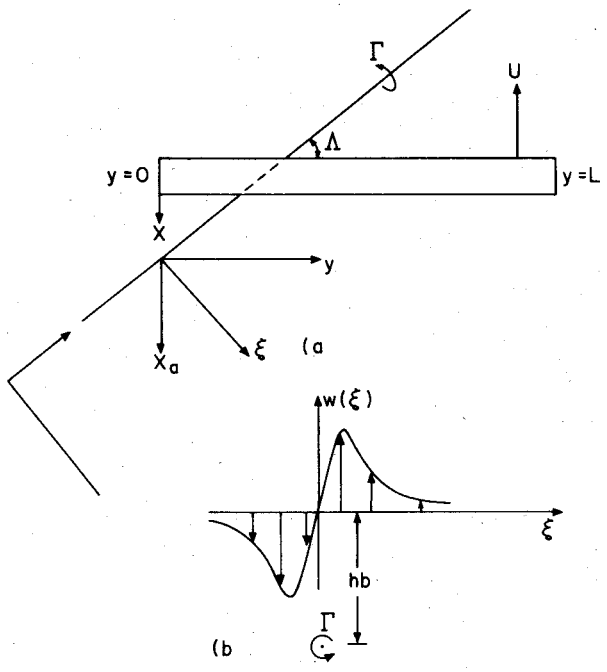

Fig. 1 Model interaction geometry and vortex upwash induced on flight plane.

The next step in the present analysis is to use this two-dimensional pressure field solution in a spanwise Fourier superposition to model the loading on a rotating rectangular blade of length L. The magnitude of the constructed spanwise loading increases linearly from zero at the hub to the full two-dimensional value at the tip; therefore, the Mach number and reduced frequency in the expression for the three-dimensional loading actually represent values of Mach number and reduced frequency at the tip. Since a rotating helicopter blade sees a freestream given approximately by the spanwise linear relation $U(y)=\Omega by$, the constructed triangular loading should model actual magnitudes of unsteady sectional loadings quite well, except near the blade tip and near the hub where complex finite-span effects introduce further complications not addressed here. The model, therefore, does not account for such forward-flight effects as nonzero unsteady lift at the hub position or local freestream sweep. These refinements should be included in future fundamental extensions of the present theory.

The model neglects the true rotational effects of acoustic sources on the radiated field [the second term of Lowson's[7] Eq. (16)] and also the spanwise variation of reduced frequency $\omega b/U$ for $U(y)=\Omega by$, $0<y<L$); yet, it represents an improvement on Widnall's model[1] in that the acoustic contribution of inboard sections is reduced rationally. The three-dimensional aerodynamic model in Ref. 1 used a spanwise superposition to yield a box-shaped loading acting over an "effective blade length." Although this model made predictions that agreed with experiment, there was no rational way to choose the effective blade length. In the present model this difficulty is removed by assuming that the unsteady loading drops off continuously from tip to hub.

We therefore assume that all blade sections pass rectilinearly over the vortex, so that the angle Λ stays constant during the interaction. This simplification is justified for $\omega/\Omega\gg 1$ or by the equivalent requirement of $(\omega b/U)(L/b)\gg 1$ (here L is dimensional) for moderate tip Mach numbers. Amiet[8] has discussed the validity of a similar assumption of local rectilinear motion for blade sections of a rotor cutting through atmospheric turbulence.

Our model also assumes that chordwise unsteadiness dominates finite-span effects at all spanwise blade sections. Although as the noncompactness of the unsteady loading is increased this may be true over most of the span, there always exists a small region near the tip where three-dimensional effects are large and where the actual loading is expected to vanish as $\sqrt{L-y}$. A more sophisticated treatment than that presented here is required to model properly the strength and

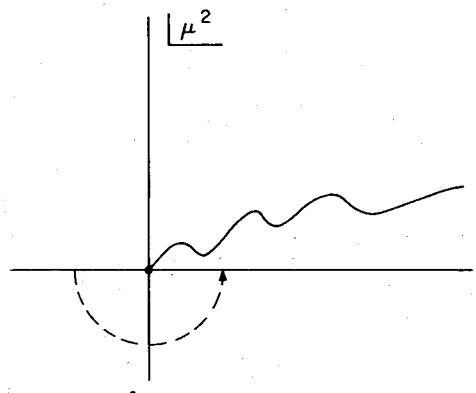

Fig. 2 Cut μ^2 plane and path of analytic continuation.

phase of tip region dipoles, and is the subject of a forthcoming paper by the authors.

Following the construction of the acoustic source, we calculate the corresponding three-dimensional pressure field, from which we then compute the theoretical acoustic far field for an arbitrary tone by the method of stationary phase. The solution is found to break down for supersonic trace speeds ($\sin\Lambda < M$), so that it may be applied only for the subsonic trace-speed case ($\sin\Lambda > M$). However, the latter is well known to include most typically large-Λ interactions observed for single-rotor helicopters. Finally, we evaluate the frequency integral in closed form (sum up the effect of all of the gusts) and obtain an expression for the acoustic pulse at an arbitrary spatial position for a rectangular blade of length L rotating over a potential vortex.

Farassat[9] has reported on a number of acoustic models, some compact and others noncompact, that workers have developed to predict acoustic radiation from rotating blades. These models, however, require that unsteady blade loads be provided for the acoustic calculation (either by experiments or by more exact numerical aerodynamic calculations); therefore, although they are more accurate, since they may make few aerodynamic simplifying assumptions, the acoustic formulas presented in Ref. 9 are not immediately applicable to make noise predictions in particular situations of interest for which a time history of unsteady loading is unknown. The theory developed here predicts both the unsteady loading and the resulting acoustic field. Since the expression for the sound pulse derived contains only elementary functions, it could be used readily to plot an estimate of the three-dimensional directivity of peak acoustic pressures.

Formulation

Figure 1a shows the geometry of the interaction considered. The potential vortex of strength Γ is in the still fluid from the point of view of an observer on the ground. It is located a distance h below the flight plane and interacts at an angle Λ with a blade of finite span L and tip speed $U=\Omega Lb$. All distances, including L and h, have been nondimensionalized with respect to the blade semichord b.

The vortex-induced upwash on the flight plane shown in Fig. 1b is given by Biot-Savart's law,

$$w(\xi)=\frac{\Gamma/b}{2\pi}\frac{\xi}{\xi^2+h^2} \tag{1}$$

By Fourier's theorem, we may express this function as a sum of sinusoidal upwash gusts, also horizontally motionless relative to the air,

$$w(\xi)=\int_{-\infty}^{\infty} dk e^{-ik\xi} W(k) \tag{2}$$

where $W(k)$ is the amplitude-phase function of each Fourier component. With $\xi=x_a\cos\Lambda+y\sin\Lambda$, where the subscript a denotes the acoustic reference frame, we may evaluate $W(k)$ by inverting the Fourier transform in Eq. (2),

$$W(k)=\iint_{-\infty}^{\infty}\frac{dx_a dy}{(2\pi)^2} w(x_a\cos\Lambda+y\sin\Lambda)\exp(ik_x x_a+ik_y y)$$

$$=\delta(k_y-k_x\tan\Lambda)\frac{W(k_x/\cos\Lambda)}{\cos\Lambda} \tag{3}$$

from which

$$w(x_a\cos\Lambda+y\sin\Lambda)=\iint_{-\infty}^{\infty} dk_y dk_x W(k)\exp(-ik_x x_a-ik_y y)$$

$$=\int_{-\infty}^{\infty} dk_x \frac{W(k_x/\cos\Lambda)}{\cos\Lambda}\exp(-ik_x x_a-ik_x\tan\Lambda y) \tag{4}$$

If we now call $bx_a=bx-Ut$, where x is fixed on the wing, we find, with $W(k_x/\cos\Lambda)/\cos\Lambda=w_0(k_x/\cos\Lambda)$ in Eq. (4), that

$$w(x_a\cos\Lambda+y\sin\Lambda)=\int_{-\infty}^{\infty} dk_x w_0\left(\frac{k_x}{\cos\Lambda}\right)$$

$$\times\exp\left(ik_x\frac{Ut}{b}-ik_x x-ik_x\tan\Lambda y\right) \tag{5}$$

The function w_0 stands for the amplitude-phase relation of gusts convected at speed U in the wing reference frame. The gust frequency ω, therefore, is $k_x U/b$ and the chordwise wave number k_x may be interpreted as $\omega b/U$, the reduced frequency. The spanwise wave number k_y is $k_x\tan\Lambda$. If $P(\bar{r}, t; k_x)$ denotes the acoustic field of a tone of frequency ω due to the interaction of the blade with a single gust, the acoustic pulse $p(\bar{r},t)$ due to blade-vortex interaction may be calculated by adding all of the tone solutions,

$$p(\bar{r},t)=\int_{-\infty}^{\infty} dk_x P(\bar{r},t;k_x) \tag{6}$$

We may specify the time origin of the transient interaction to correspond to blade position $x_a=0$, so that positive values of source time $\tau>0$ correspond with $x_a<0$ and negative values $\tau<0$ with $x_a>0$. Because of this sign difference between the spatial and time scale, care should be taken to use $w_0(-k_x/\cos\Lambda)$, rather than $w_0(k_x/\cos\Lambda)$, in Eq. (6) to otain the time history of the acoustic pressure at a point in space.

Leading Edge Passing Through an Oblique Gust in Two Dimensions

The pressure field for infinite-span airfoil passing through an oblique gust is now calculated. This pressure field agrees with the leading-edge contribution to the far-field acoustic pressure calculated in Ref. 3 by letting $\sqrt{x^2+Z^2}\to\infty$ and using steepest descents. We find that the pressure at an arbitrary point (x,z) in fact has the same form as the far-field pressure.

From Ref. 3, Eq. (14), the leading-edge contribution to the two-dimensional pressure field for an infinite-span airfoil passing through an oblique gust is

$$P_{2\text{-D}}=\frac{-\rho_0 w_0 U}{2\pi\sqrt{1-M^2}}\frac{1}{\sqrt{k_x/(1-M^2)+\mu}}\frac{Z}{|Z|}$$

$$\times\exp\left(i\omega t-ik_y y+\frac{ik_x M^2 x}{1-M^2}\right)$$

$$\times\int_C\frac{d\lambda\exp\{-\sqrt{\lambda^2-\mu^2}\,|Z|-i\lambda x\}}{\sqrt{\lambda-\mu}} \tag{7}$$

where ρ_0 and M are the freestream density and Mach number, respectively, $Z=\sqrt{1-M^2}z$, and μ is given by

$$\mu=\sqrt{\frac{k_x^2M^2}{(1-M^2)^2}-\frac{k_y^2}{1-M^2}}=\frac{k_x|\tan\Lambda|}{(1-M^2)}\left[\frac{M^2}{\sin^2\Lambda}-1\right]^{1/2} \tag{8}$$

which is real for $\sin\Lambda<M$ (or $\tan\Lambda<M/\sqrt{1-M^2}$). C is a complex contour of integration in the complex λ plane passing over the branch point at $\lambda=+\mu$ and below that at $\lambda=-\mu$. For $\sin\Lambda<M$ we initially assume $\mu=\mu_r-i\epsilon$, $1\gg\epsilon>0$, in order to satisfy the radiation condition at ∞. C is then such that $|\mathrm{Im}\lambda|<\epsilon$. For $\mu^2<0$, we take $\mu=-i\sqrt{-\mu^2}$, so that the horizontal strip through which the contour C runs becomes wider. It is convenient to think of μ^2 as a complex variable in the complex μ^2 plane; in order to insure that $\mu=-i\sqrt{-\mu^2}$ for $\mu^2<0$, a cut is drawn above the positive real axis (Fig. 2). To evaluate the integral in Eq. (7), we first assume that $\mu^2<0$ and then analytically continue the final result in the μ^2 plane (Fig. 2, dotted line) to the positive real axis. A similar integral is treated in Ref. 10.

With $a^2=-\mu^2$, we make the change of variable

$$\lambda=a\sinh\beta \tag{9a}$$

$$d\lambda=a\cosh\beta d\beta \tag{9b}$$

and let $\theta=\tan^{-1}Z/x$, $r=\sqrt{x^2+Z^2}$ in Eq. (7). The integral then becomes, in the β plane,

$$\sqrt{a}\int_{-\infty}^{\infty} d\beta\sqrt{\sinh\beta-i}\exp[-iar\sinh(\beta-i\theta)] \tag{10}$$

Since

$$\sqrt{\sinh\beta-i}=\cos(\theta/2)\sqrt{\sinh(\beta-i\theta)-i}$$
$$-\sin(\theta/2)\sqrt{-\sinh(\beta-i\theta)-i}$$

we may now make the change

$$s=\sinh(\beta-i\theta) \tag{11a}$$

$$ds=\cosh(\beta-i\theta)\,d\beta \tag{11b}$$

to obtain

$$\sqrt{a}\cos\frac{\theta}{2}\int_{\sinh(-\infty-i\theta)}^{\sinh(\infty-i\theta)}\frac{ds}{\sqrt{s+i}}\exp(-iars)$$
$$-\sqrt{a}\sin\frac{\theta}{2}\int_{\sinh(-\infty-i\theta)}^{\sinh(\infty-i\theta)}\frac{ds}{\sqrt{-s+i}}\exp(-iars) \tag{12}$$

where the cuts in the complex s plane extend from $s=i$ to $s=i\infty$ and from $s=-i$ to $s=-i\infty$. The quantity ar is positive, so that both integrals in Eq. (12) may be deformed to the lower half s plane. Since the second integrand is analytic there, the second integral contributes zero. The contribution of the first integral in Eq. (12) is readily calculated to be

$$\frac{2\sqrt{\pi}\cos(\theta/2)}{\sqrt{r}}\exp\left(\frac{-i\pi}{4}-ar\right) \tag{13}$$

which, upon analytic contribution to the positive μ^2 real axis, and substitution back into Eq. (6), yields the result sought,

$$P_{2\text{-D}}=\frac{\mp\rho_0 w_0 U}{\sqrt{\pi}\sqrt{1-M^2}}\frac{1}{\sqrt{\mu+k_x/(1-M^2)}}\frac{\cos(\theta/2)}{\sqrt{r}}$$
$$\times\exp\left[i\left\{\omega t-k_y y+\frac{k_x M^2 x}{1-M^2}-\frac{\pi}{4}-\mu r\right\}\right] \tag{14}$$

The loading on the airfoil due to the passage through the gust may be obtained from Eq. (14) by letting $z=\theta=0$ ($r=x>0$). The pressure field decays exponentially for $\sqrt{-\mu^2}=a>0$ and there is no acoustic field. The airfoil loading then physically represents a disturbance traveling subsonically through the still fluid. For each chordwise position, acoustic sources distributed along the infinite span cancel each other perfectly in the far field.

Rotating Blade of Finite Length Passing Over a Potential Vortex

A spanwise superposition of the basic two-dimensional loading [$\theta=0$ in Eq. (14)] is performed to model the three-dimensional surface pressure distribution on a rotating blade of length L passing through an oblique gust. The constructed loading will have its full two-dimensional magnitude given in Eq. (7) at $y=L$ and will decrease linearly to zero at $y=0$.

We define the three-dimensional pressure field $P_{3\text{-D}}(x,y,Z,t;k_x)$ due to the passage of a rotating blade of length L (nondimensionalized by the blade semichord b) through an oblique gust. $P_{3\text{-D}}$ satisfies the linearized convected wave equation in three dimensions [Ref. 2, Eq. (1)]. We let

$$P_{3\text{-D}}(x,y,Z,t)=P_*(x,y,Z)\exp\left(i\omega t+\frac{ik_x M^2 x}{1-M^2}\right) \tag{15}$$

and $Y=\sqrt{1-M^2}y$, so that P_* satisfies

$$P_{*xx}+P_{*YY}+P_{*ZZ}+\left(\frac{k_x M}{1-M^2}\right)^2 P_*=0 \tag{16}$$

subject to the boundary condition

$$P_*(x,Y,0+)$$
$$=\begin{cases} Y/L\sqrt{1-M^2}P_{*2\text{-D}}(x,y,0+) & \text{for } 0<Y<\sqrt{1-M^2}L \\ 0 & \text{otherwise}\end{cases} \tag{17}$$

where $P_{*2\text{-D}}(x,y,0+)$ is seen from Eq. (14), with $k_y=k_x\tan\Lambda$, to be

$$P_{*2\text{-D}}(x,Y,0+)$$
$$=-\frac{\rho_0 w_0 U\exp(-i\pi/4-i\mu x-ik_x\tan\Lambda Y/\sqrt{1-M^2})}{\sqrt{\pi}\sqrt{1-M^2}\sqrt{\mu+k_x(1-M^2)}\sqrt{x}} \tag{18}$$

We now define the transform pair

$$P_*(x,Y,Z)=\int_{-\infty}^{\infty}\int\frac{d\lambda_1 d\lambda_2}{(2\pi)^2}\bar{P}(\lambda_1,\lambda_2;Z)\exp(-i\lambda_1 x-i\lambda_2 Y) \tag{19a}$$

$$\bar{P}(\lambda_1,\lambda_2;Z)=\int_{-\infty}^{\infty}\int dx\,dY P_*(x,Y,Z)\exp(i\lambda_1 x+i\lambda_2 Y) \tag{19b}$$

Transforming Eq. (16) and solving the resulting ordinary differential equation, we obtain

$$\bar{P}(\lambda_1,\lambda_2;Z\pm)=\pm\bar{P}(\lambda_1,\lambda_2,0+)e^{\mp Z\sqrt{\lambda_1^2+\lambda_2^2-K^2}} \tag{20}$$

where we have called $K=k_x M/(1-M^2)$ for convenience. From Eqs. (19b) and (18), it follows that

$$\bar{P}(\lambda_1,\lambda_2,0+)=F(\lambda_1)G\left(\lambda_2-\frac{k_x\tan\Lambda}{\sqrt{1-M^2}}\right) \tag{21}$$

where

$$F(\lambda_1)=-\frac{\rho_0 w_0 U}{\sqrt{1-M^2}\sqrt{\mu+k_x/(1-M^2)}}\frac{1}{\sqrt{\lambda_1-\mu}} \tag{22a}$$

and

$$G\left(\lambda_2-\frac{k_x\tan\Lambda}{\sqrt{1-M^2}}\right)$$
$$=\int_0^{\sqrt{1-M^2}L}dY\frac{Y}{\sqrt{1-M^2}}\exp\left[iY\left(\lambda_2-\frac{k_x\tan\Lambda}{\sqrt{1-M^2}}\right)\right] \tag{22b}$$

We now translate the solution, obtained by substituting Eqs. (20-22) into Eq. (19a), from the blade reference frame to the still-fluid reference frame. In the following $bx_a=bx-Ut$; let

$$\lambda_1=b\tilde{\lambda}_1+k_x M^2/(1-M^2) \tag{23a}$$

$$\lambda_2=b\tilde{\lambda}_2/\sqrt{1-M^2} \tag{23b}$$

and revert to the original unstretched variables y and z. Introducing the following $\omega'-t$ δ function relation, Eq. (21) becomes

$$P_{3\text{-D}}(x_a,y,z,t)=\int_{-\infty}^{\infty}\int\frac{b^2 d\tilde{\lambda}_1 d\tilde{\lambda}_2}{(2\pi)^2\sqrt{1-M^2}}$$
$$\times\int_{-\infty}^{\infty}d\omega' e^{i\omega' t-i\tilde{\lambda}_1 bx_a-i\tilde{\lambda}_2 by}\exp\left(-ibz\sqrt{\frac{\omega'^2}{c_0^2}-\tilde{\lambda}_1^2-\tilde{\lambda}_2^2}\right)$$
$$\times\delta[\omega'-(\omega-\tilde{\lambda}_1 U)]F\left(b\tilde{\lambda}_1+\frac{k_x' M^2}{1-M^2}\right)G\left(b\tilde{\lambda}_2-\frac{k_x'\tan\Lambda}{\sqrt{1-M^2}}\right) \tag{24}$$

where $k_x'=(\omega'+\tilde{\lambda}_1 U)b/U$.

Next, we express the δ function in Eq. (25) in terms of one of its well-known limiting forms, $\delta(a)=\lim_{\epsilon\to 0}(1/\pi)\epsilon/(\epsilon^2+a^2)$ and interchange the orders of $\tilde{\lambda}_1$, $\tilde{\lambda}_2$ integration with the ω' integral. Then we approximate the $\tilde{\lambda}_1$, $\tilde{\lambda}_2$ integrals for $\sqrt{x_a^2+y^2+z^2}\to\infty$ by the method of stationary phase.[11] Finally, we change the limit-δ function back to its exact form, evaluate the ω' integral, and obtain the acoustic field for a rotating blade of length L passing through a stationary gust. M is the tip Mach number.

$$P_{3\text{-D}}(x_a,y,z,t)=\left\{-i\rho_0 w_0 UM\sqrt{1-M^2}\exp\left[\frac{i\omega(t-br_a/c_0)}{1+Mx_a/r_a}\right]\right\}$$
$$\div\left\{2\pi Lr_a\sqrt{1+|\tan\Lambda|\sqrt{\frac{M^2}{\sin^2\Lambda}-1}}\right\}\frac{D_{3\text{-D}}\left(\frac{x_a}{r_a},\frac{y}{r_a},\frac{z}{r_a}\right)}{\left(1+\frac{Mx_a}{r_a}\right)^2} \tag{25a}$$

where the predicted three-dimensional acoustic directivity pattern $D_{3\text{-D}}$ [not including the $(1+Mx_a/r_a)^{-2}$ term] is

$$D_{3\text{-D}}\left(\frac{x_a}{r_a},\frac{y}{r_a},\frac{z}{r_a}\right)=\frac{z/r_a}{\left(\tan\Lambda-\frac{My/r_a}{1+Mx_a/r_a}\right)^2}$$
$$\times\frac{1}{\sqrt{\frac{M(M+x_a/r_a)}{1+Mx_a/r_a}-|\tan\Lambda|\sqrt{\frac{M^2}{\sin^2\Lambda}-1}}}$$
$$\times\int_0^{L\left(\tan\Lambda-\frac{My/r_a}{1+Mx_a/r_a}\right)}dy\,y\exp(-ik_x y) \tag{25b}$$

The grouping $1+Mx_a/r_a$, which appears explicitly in the denominator of Eq. (25a) and as part of the exponential's argument, accounts respectively for the familiar forward enhancement due to motion in the $-x_a$ direction and for the position-dependent Doppler shift. The direction cosines x_a/r_a, y/r_a, z/r_a, and the distance $r_a=\sqrt{x_a^2+y^2+z^2}$ in Eqs. (25) specify the position of the observer in three-dimensional space.

The expression on the right side of Eq. (25b) stands as is for $M/\sin\Lambda>1$, i.e., for supersonic trace speeds of the disturbance. For subsonic trace speed of load fronts ($\sin\Lambda>M$), we recall that $\mu=-i\sqrt{-\mu^2}$; thus the following change should be made:

$$\sqrt{(M^2/\sin^2\Lambda)-1}=-i\sqrt{1-(M^2/\sin^2\Lambda)} \tag{26}$$

For supersonic case, the term inside the radical on the right side of Eq. (25b) blows up in the direction given by

$$\frac{x_a}{r_a}=-\left[\frac{M-(|\tan\Lambda|/M)\sqrt{(M^2/\sin^2\Lambda)-1}}{1-|\tan\Lambda|\sqrt{(M^2/\sin^2\Lambda)-1}}\right] \tag{27}$$

This is the direction taken by acoustic rays originating at the line of intersection of the downstream part of a typical Mach cone and the x_a-y plane. The breakdown of the leading-edge solution in this direction can be explained as follows: since the chord extends downstream to infinity, in the above operations we have in fact tried to calculate the acoustic field of a distribution of supersonic sources that is infinite in extent; the surfaces of the associated system of Mach cones do not interfere and so even those far from the leading edge have a substantial acoustic effect. Therefore, we cannot interpret the three-dimensional acoustic field as emanating from an equivalent complicated source concentrated at the origin (the essential assumption in the stationary-phase approximation) and thus we cannot calculate it by the present method. The following analysis is limited to the subsonic trace-speed case, which describes most interactions observed in single-rotor helicopters.

Implicit in the work here up to Eqs. (25) was the assumption that the frequency ω (and so also k_x) has a positive value. With the substitution of Eq. (26), Eqs. (25) indicate that $P_{3\text{-D}}$

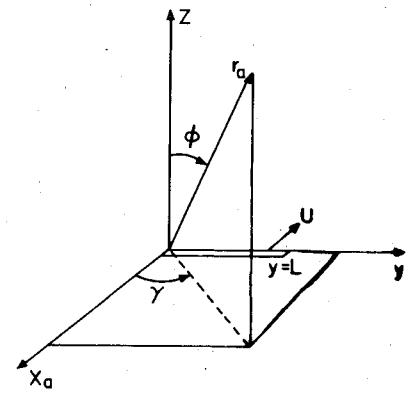

Fig. 3 Spherical coordinate system fixed in the still fluid defining observer position in three dimensions.

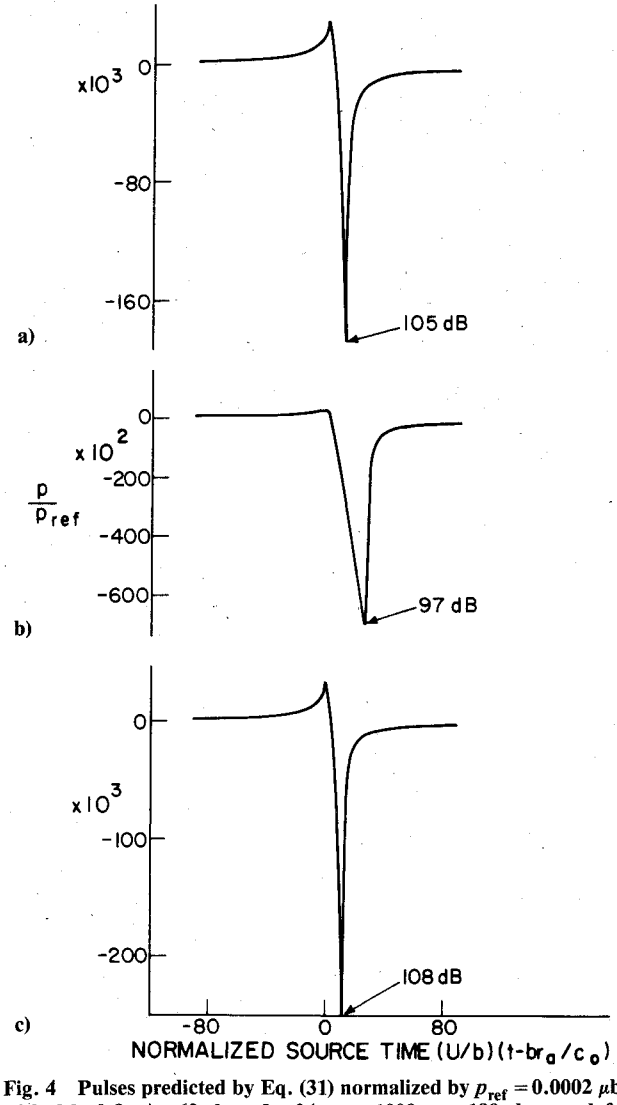

Fig. 4 Pulses predicted by Eq. (31) normalized by $p_{\text{ref}}=0.0002$ μbar with $M=0.8$, $\Lambda=62$ deg, $L=24$, $r_a=1000$, $\gamma=180$ deg, and for: a) $h=0.5$, $\phi=65$ deg; b) $h=0.5$, $\phi=30$ deg; c) $h=0.1$, $\phi=65$ deg.

is given essentially by the product of a complex constant

$$C=-i\Big/\sqrt{1-i\,|\tan\Lambda|\left\{1-\frac{M^2}{\sin^2\Lambda}\right\}^{1/2}}$$

$$\times 1\Big/\left\{\frac{M(\sin\phi\cos\gamma+M)}{1+M\sin\phi\cos\gamma}+i\,|\tan\Lambda|\sqrt{1-\frac{M^2}{\sin^2\Lambda}}\right\}^{1/2} \quad (28)$$

and a function $f(k_x)$. Equation (6) therefore becomes (*denotes complex conjugate):

$$p(\bar{r}_a,t)=\frac{\rho_0\Gamma c_0M^2\sqrt{1-M^2}\cos\phi}{8\pi^2\cos\Lambda bLr_a(1+M\sin\phi\cos\gamma)^2}$$

$$\times 1\Big/\left(\tan\Lambda-\frac{M\sin\phi\sin\gamma}{1+M\sin\phi\cos\gamma}\right)^2$$

$$\times\left\{C^*\int_0^\infty dk_x f(-k_x)+C\int_0^\infty dk_x f(k_x)\right\} \quad (29)$$

where the integrands contain $w_0(-k_x/\cos\Lambda)$, which for the potential vortex in Fig. 1 may be readily calculated to be

$$w_0\left(-\frac{k_x}{\cos\Lambda}\right)=-\frac{i\Gamma/b}{4\pi\cos\Lambda}\frac{k_x}{|k_x|}\exp(-h\,|k_x|/\cos\Lambda) \quad (30)$$

With Eq. (30), the integrals in Eq. (29) may be evaluated to obtain the acoustic pulse, in terms of retarded time (or source time) τ, at an arbitrary point in space,

$$p(\bar{r}_a,t)=\frac{\rho_0\Gamma c_0M^2\sqrt{1-M^2}\cos\phi}{4\pi^2\cos\Lambda bLr_a(1+M\sin\phi\cos\gamma)^2}\frac{1}{\left(\tan\Lambda-\frac{M\sin\phi\sin\gamma}{1+M\sin\phi\cos\gamma}\right)^2}\left\{L\left(\tan\Lambda-\frac{M\sin\phi\sin\gamma}{1+M\sin\phi\cos\gamma}\right)Re(C)\right.$$

$$+\left|C\left(\frac{(U/b)\tau}{1+M\sin\phi\cos\gamma}+\frac{ih}{\cos\Lambda}\right)\right|\left[\cos\left\{\arg\left[C\left(\frac{(U/b)\tau}{1+M\sin\phi\cos\gamma}+\frac{ih}{\cos\Lambda}\right)\right]\right\}\right.$$

$$\times\log\left|\frac{\frac{(U/b)\tau}{1+M\sin\phi\cos\gamma}-L\left(\tan\Lambda-\frac{M\sin\phi\sin\gamma}{1+M\sin\phi\cos\gamma}\right)+\frac{ih}{\cos\Lambda}}{\frac{(U/b)\tau}{1+M\sin\phi\cos\gamma}+\frac{ih}{\cos\Lambda}}\right|$$

$$\left.\left.-\arg\left(\frac{\frac{(U/b)\tau}{1+M\sin\phi\cos\gamma}-L\left(\tan\Lambda-\frac{M\sin\phi\sin\gamma}{1+M\sin\phi\cos\gamma}\right)+\frac{ih}{\cos\Lambda}}{\frac{(U/b)\tau}{1+M\sin\phi\cos\gamma}+\frac{ih}{\cos\Lambda}}\right)\sin\left\{\arg\left[C\left(\frac{(U/b)\tau}{1+M\sin\phi\cos\gamma}+\frac{ih}{\cos\Lambda}\right)\right]\right\}\right]\right\} \quad (31)$$

where we have used the spherical coordinate system shown in Fig. 3 to indicate the observer position; there $x_a/r_a=\sin\phi\cos\gamma$, $y/r_a=\sin\phi\sin\gamma$, and $z/r_a=\cos\phi$.

The final result is real, as it should be since neither the free-space wave equation governing p nor the original vortex-induced upwash [Eq. (1)] have complex coefficients. To apply it, we have chosen physical parameters corresponding approximately to those of the two-bladed, 3636 kg (8000 lb) Hughes model UH-1H helicopter. The constant blade semichord is taken as equal to 0.305 m (1 ft); a nondimensional blade length L of 24 is used [for an actual rotor diameter of 14.63 m (48 ft). The steady sectional loading on each blade is assumed to have a maximum value $L_{\max}=\rho_0c_0M\Gamma$ at the tip and to decrease linearly from this to zero at the hub; for $M=M_{\text{tip}}=0.8$, Γ is about 14.77 m^2/s (159 ft^2/s). STP values of air density and sound speed are assumed in the calculations, and the standard reference pressure of 0.0002 μbar is used for normalization.

Figures 4a and 4b show plots of Eq. (30) for $h=0.5$ (vortex ¼ chord below flight plane) with $M=0.8$, $\Lambda=62$ deg (such that $M_{\text{eff}}=0.91$), at the two distinct spatial positions given by $\phi=65$ and 30 deg, both with $r_a=1000$ and $\gamma=180$ deg.

Referring to the coordinate system in Fig. 3, one would expect: 1) greater frequency shifting (resulting in a sharper signature) at $\phi=65$ deg than at $\phi=30$ deg; 2) higher levels for all the tones making up a louder signal at $\phi=65$ deg, because the forward enhancement effect is greater at the lower elevation (for $\phi=90$ deg, however, the pressure is zero). The pulses in Figs. 4a and 5b indicate that the model is able to predict both effects. When compared to Fig. 4a, Fig. 4c illustrates the acoustic consequence of reducing the vertical blade-vortex separation in the model. The pulse is richer in high-frequency components than for $h=0.5$ (it is somewhat sharper), and the predicted peak pressure has an expectedly higher value due physically to a greater time rate of change of the vortex-induced blade loading.

It is interesting to note that the present noncompact theory predicts an increase of only 3 dB when h is reduced five-fold from 0.5 to 0.1; a similar change in h typically results in peak pressure increments of 15 dB or more, when M is low enough to permit analysis by a compact model, e.g., Ref. 2. The reason for the difference in sensitivity to blade-vortex separation may be traced to differences in the calculated spectra. The compact model in Ref. 2 predicts a spectrum (not counting the w_0 part) that increases indefinitely with frequency. The noncompact theory developed here predicts that the same part of the spectrum, i.e., not counting w_0, levels off to a constant value. We expect, therefore, that extension of compact models to include very small h cases results in predictions of peak pressures that are higher than those obtained using the more relevant noncompact theory.

The predicted pulses contain the familiar features of blade-slap signatures attributed to blade-vortex interaction: two peaks are present, first one small in magnitude and positive, and then a large negative one. Qualitatively, the pulses seem to reproduce well blade-vortex noise waveforms measured by other investigators, e.g., Boxwell et al.[12] Unfortunately, lack of precise experimental knowledge of interaction parameters, such as h and Λ, makes a comparison of measured and predicted amplitudes difficult.

Equations (25) show that the predicted amplitude-phase relation for tones is a complicated function of position unless $k_xL\ll 1$, a condition not expected to be met by high-energy spectral components of the radiated pulse when h is reasonably small and for which the model developed here is not valid. A great deal of "hard-to-visualize" cancellation or reinforcement occurs throughout, so that directivities of tone

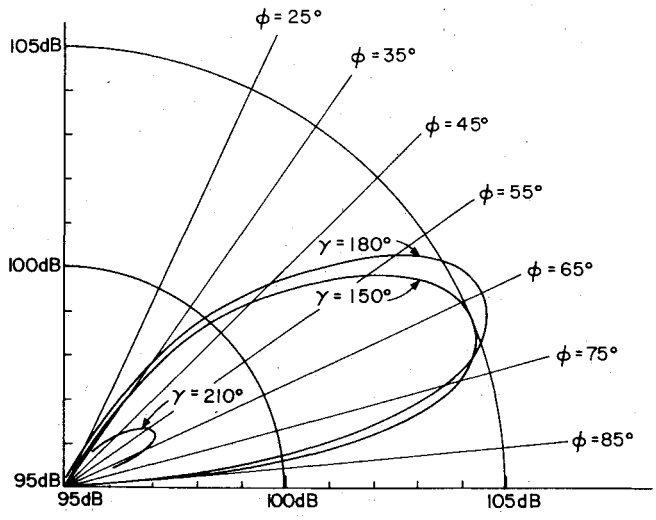

Fig. 5 Predicted three-dimensional directivity pattern of peak acoustic pressures with $M=0.8$, $\Lambda=62$ deg, $h=0.5$, $L=24$.

amplitudes could be deceptive indicators of peak-pressure values without knowledge of how the tones actually add up in space. Since we have a closed-form solution for the pulse, however, a calculation of peak pressures may now be carried out at a number of spatial positions without too much expense.

With $M=0.8$, $\Lambda=62$ deg, and $h=0.5$, Fig. 5 shows a plot of some peak pressures at spatial positions within the solid sector given by $25<\phi<85$ and $150<\gamma<210$ deg, i.e., ± 30 deg about $\gamma=180$ deg, the azimuth in line with the flight direction. Large amplitudes should be expected in this region due to forward beaming. We note that for $\gamma=150$ and 180 deg substantial differences exist in predicted values of peak pressure as ϕ is increased from 25 to 85 deg, whereas for $\gamma=210$ deg only a small change is present. We attribute this feature of the peak-pressure directivity pattern to spatial differences in the amount of local cancellation or reinforcement of tones, which in turn have the complicated phase-frequency relationship given by the integral term in Eq. (25).

Summary and Conclusions

The contributions of this paper are basically:

1) The closed-form evaluation of the theoretical two-dimensional pressure field for a leading-edge flat-plate airfoil passing subsonically through a gust.

2) A closed-form solution for the pulse radiated by a leading-edge helicopter blade of length L passing subsonically over a potential vortex. The interaction angle Λ must be large enough for predicted load fronts to have an absolute trace speed less than sonic. The model could be used to make predictions of noise from single-rotor helicopters for which large interaction angles are commonly observed. For supersonic trace speeds the model breaks down.

Although result 1 served mostly as a stepping stone to result 2 in the development, it is interesting in itself. A close analogy has been known to exist between the problem of an airfoil passing through a parallel gust ($\Lambda=0$) for $M>1$ and the classical Sommerfeld diffraction of an incident plane wave by a semi-infinite flat plate. Both problems have a closed-form solution at an arbitrary field point. Result 1 shows that a closed-form solution exists for the airfoil problem not just for $M>1$, but also for $M<1$.

Result 2 for the theoretically predicted pulse reproduces the basic shape of measured signals due to helicopter blade-vortex interaction. Experiments with precise control over h and Λ are yet needed to determine just how well the theory developed here predicts peak values of amplitude. If future work indicates good agreement, then the simplicity of result 2 would allow inexpensive predictions of three-dimensional directivities of peak acoustic pressures.

In applying result 2 for subsonic trace speeds, we expect the radiation field of each tone making up the pulse to be due to spanwise finite-length effects rather than to the presence of the leading edge. This must be so since result 1 proved that the two-dimensional acoustic field radiated by the leading edge alone vanishes for $\sin\Lambda>M$.

Although for the constructed three-dimensional loading acoustic sources inboard should have reasonably correct phase and magnitude, those farther outboard, particularly near the tip, probably do not. In our aerodynamic model we simply cut off the loading abruptly at the tip, where in reality the relatively smooth $\sqrt{L-y}$ behavior is known to occur; we have therefore overestimated the strength of tip region dipoles, and have neglected other complex three-dimensional effects.

Acknowledgment

This work was supported by NASA Grant NSG-2142.

References

[1] Widnall, S. E., "Helicopter Noise due to Blade-Vortex Interaction," *Journal of the Acoustical Society of America*, Vol. 50, No. 1, Pt. 2, 1971, pp. 354-365.

[2] Filotas, L. T., "Theory of Airfoil Response in a Gusty Atmosphere—Part I, Aerodynamic Transfer Function," University of Toronto, Canada, UTIAS Rept. 139, Oct. 1969.

[3] Martinez, R. and Widnall, S. E., "Unified Aerodynamic-Acoustic Theory for a Thin Rectangular Wing Encountering a Gust," *AIAA Journal*, Vol. 18, June 1980, pp. 636-645.

[4] Adamczyk, J. J., "The Passage of an Infinite Swept Airfoil through an Oblique Gust," NASA CR-2395, May 1974.

[5] Amiet, R. K., "High-Frequency Thin Airfoil Theory for Subsonic Flow," *AIAA Journal*, Vol. 14, Aug. 1976, pp. 1076-1082.

[6] Landahl, M. T., *Unsteady Transonic Flow*, Pergamon Press, New York, 1961, pp. 28-29.

[7] Lowson, M. V., "The Sound Field for Singularities in Motion," *Proceedings of the Royal Society of London*, Vol. A286, Aug. 1965, pp. 559-572.

[8] Amiet, R. K., "Noise Produced by Turbulent Flow into a Propeller or Helicopter Rotor," *AIAA Journal*, Vol. 15, March 1977, pp. 307-308.

[9] Farassat, F., "Linear Acoustic Formulas for Calculation of Rotating Blade Noise," *AIAA Journal*, Vol. 19, Sept. 1981, pp. 1122-1130.

[10] Carrier, G. F., Krook, M., and Pearson, C. E., *Functions of a Complex Variable, Theory and Technique*, McGraw-Hill Book Co., New York, 1966, p. 93.

[11] Whitham, G. B., *Linear and Nonlinear Waves*, John Wiley & Sons, New York, 1974, p. 382.

[12] Boxwell, D. A., Schmitz, F. H., and Hanks, M. L., "In-Flight Far-Field Measurements of Helicopter Impulsive Noise," Paper presented at First European Rotorcraft and Powered Lift Aircraft Forum, Sept. 22-24, 1975.